

## Electronic Supplementary Information (ESI)

### Gallate-MOF derived CoS<sub>2</sub>/C composites as an accelerated catalyst for room-temperature sodium–sulfur batteries

Qiuyang Ma,<sup>a,b</sup> Jing Ai,<sup>a,b</sup> Haoda Zou,<sup>a,b</sup> Hengli He,<sup>a,b</sup> Zhongyuan Li,<sup>a,b</sup> Jawayria Mujtaba,<sup>\* a,b</sup> and Zhen Fang<sup>\* a,b,c</sup>

<sup>a</sup> College of Chemistry and Materials Science, Key Laboratory of Electrochemical Clean Energy of Anhui Higher Education Institutes, Anhui Normal University, Wuhu 241000, PR China

<sup>b</sup> Key Laboratory of Functional Molecular Solids, Ministry of Education, Anhui Normal University, Wuhu 241000, PR China

<sup>c</sup> Anhui Provincial Engineering Laboratory for New-Energy Vehicle Battery Energy-Storage Materials, Wuhu 241000, PR China

\* Corresponding authors: [fzfsn@mail.ahnu.edu.cn](mailto:fzfsn@mail.ahnu.edu.cn); [jawayria.m@icloud.com](mailto:jawayria.m@icloud.com)

**Synthesis of Co-gallate precursor:** 1.36 g gallic acid ( $C_7H_6O_5$ ) was dissolved in solvents consist of 10 mL anhydrous ethanol solution under with vigorous stirring at room temperature. After 10 mins, 10 mL 0.05 M KOH was added and stirred vigorously. Then, 0.0364 g hexadecyl trimethyl ammonium bromide (CTAB) and 0.952 g  $CoCl_2 \cdot 6H_2O$  was separately dissolved into the above uniform solution to form a clear pink solution under stirring. Subsequently, 10 mL ethylene glycol solution was injected into the suspension under stirring for 10 min. Finally, the mixture solution was sealed in a 50 mL Teflon-lined stainless-steel and heated at  $160^\circ C$  for 12 h. After that, the obtained Co-gallate sample was washed with alcohol/distilled water, dried under  $60^\circ C$  overnight.

**Synthesis of the microprisms  $CoS_2/C$  Materials:** Typically, for the  $CoS_2/C$  composite fabrication, 100 mg Co-gallate and 1 g sulfur powder were put at each end of a quartz boat, and then heated at  $600^\circ C$  for 2 h under  $N_2$  atmosphere flow. The black product is denoted as  $CoS_2/C$ .

**Synthesis of the C Materials:** The contrast sample was synthesized by carbonizing gallic acid directly and named as C.

**Synthesis of the microprisms  $Co_3O_4/C$  Materials:** Typically, for the  $Co_3O_4/C$  composite fabrication, 100 mg Co-gallate powder were putted at a quartz boat, and then heated at  $400^\circ C$  for 2 h under  $N_2$  atmosphere flow. The black products were denoted as  $Co_3O_4/C$ .

**Synthesis of the microprisms  $CoSe_2/C$  Materials:** Typically, for the  $CoSe_2/C$  composite fabrication, 100 mg Co-gallate and 300 mg selenium powder were putted at each end of a quartz boat, and then heated at  $500^\circ C$  for 2 h under  $H_2/Ar$  atmosphere flow. The black products were denoted as  $CoSe_2/C$ .

**Synthesis of  $S@CoS_2/C$ ,  $S@Co_3O_4/C$ ,  $S@CoSe_2/C$  and  $S@C$  Composites.** The as-prepared composites ( $CoS_2/C$ ,  $Co_3O_4/C$ ,  $CoSe_2/C$  and C) and sulfur were mixed in a certain weight ratio and transferred to a tube furnace. The mixture was heated at  $155^\circ C$  for 12 h, then heated at  $200^\circ C$  for 30 min to eliminate the surface sulfur. The products were denoted as  $S@CoS_2/C$ ,  $S@Co_3O_4/C$ ,  $S@CoSe_2/C$  and  $S@C$ .

**Materials Characterization.** The phases of the as-prepared composites were

investigated by X-ray diffraction (XRD, Bruker D8). The morphologies and structure of products were characterized by Scanning electron microscopy (SEM, Hitachi 8100), transmission electron microscopy (TEM, Hitachi HT7700) and high-resolution (HR)-TEM imaging (HRTEM, Hitachi H-9500). Raman spectroscopy were collected on a Renishaw InVia (532 nm laser) and X-ray photoelectron spectroscopy (XPS) spectra data were tested on a Thermo ESCALAB250Xi spectrometer. Thermogravimetric analysis (TGA, Mettler Toledo TGA-2) can test the sulfur contents. The BET surface areas and textural properties were achieved using a Quantachrome Instruments (USA).

**Electrochemical Measurements.** The 70 wt% active materials (S@CoS<sub>2</sub>/C, S@Co<sub>3</sub>O<sub>4</sub>/C, S@CoSe<sub>2</sub>/C and S@C), 20 wt% acetylene black and 10 wt% carboxymethyl Cellulose (CMC) were homogenized mixed in water to form a slurry, and casted on the carbon coated Cu foil, then dried at 60 °C for 12 h under vacuum. In the following step, the electrodes were catted into circular disks with a diameter of 12 mm, and the average mass loading was up to 2 mg cm<sup>-2</sup>. The coin cells were assembled in an Ar-filled glovebox by using active sulfur as the cathode, Na metal as the counter electrode and glass fiber (GF/D, Whatman) as separator. The electrolyte for RT Na-S batteries was 1 M NaSO<sub>3</sub>CF<sub>3</sub> dissolved in diethylene glycol dimethyl ether (DEGDME). The galvanostatically charged-discharge experiments were tested on Neware Battery system. Cyclic voltammetry (CV, 0.1 mV s<sup>-1</sup> sweep rate over the range 0.8–2.8 V) and electrochemical impedance spectroscopy (EIS) measurements were performed on an electrochemical workstation (CHI 660E).

**Preparation of Na<sub>2</sub>S<sub>6</sub> Solution and Adsorption Test.** Sulfur and Na<sub>2</sub>S (molar ratio 5:1) were mixed in DEGDME and stirred continuously for 12 h at 80 °C until all solids were completely dissolved to obtain a dark yellowish black Na<sub>2</sub>S<sub>6</sub> solution. For the polysulfide adsorption test, 20 mg of CoS<sub>2</sub>/C or C powder was added into Na<sub>2</sub>S<sub>6</sub> solution and kept for 6 h. All the steps were completed in the glovebox. The supernatant was analyzed by UV-vis absorption spectrum.

**Symmetric-cell assembly.** The electrode was prepared by mixing active materials (CoS<sub>2</sub>/C or C) and CMC with a weight ratio of 9:1 in water, and casted on the carbon

coated Cu foil. Two identical electrodes were used as working and counter electrodes, and 25  $\mu\text{L}$  0.2 M  $\text{Na}_2\text{S}_6$  was the electrolyte. The cyclic voltammetry measurements of the symmetric cells were performed within a voltage window between -1.0 and 1.0 V with a scan rate of 50  $\text{mV s}^{-1}$ .

**Catalytic Effect Evaluation.** Sulfur and  $\text{Na}_2\text{S}$  (molar ratio 7:1) were mixed in DEGDME and stirred continuously for 12 h at 80  $^\circ\text{C}$  until all solids were completely dissolved to obtain  $\text{Na}_2\text{S}_8$  solution. Nucleation and dissolution measurements of  $\text{Na}_2\text{S}$  were performed with 0.2 M  $\text{Na}_2\text{S}_8$  2032 coin-type cells, which were assembled with the electrode containing 90 wt % of the active material ( $\text{CoS}_2/\text{C}$  or C) and 10 wt% of CMC. 25  $\mu\text{L}$  of 0.2 M  $\text{Na}_2\text{S}_8$  was dropped on the cathode, and 25  $\mu\text{L}$  of DEGDME electrolyte was added to the anode side (Na metal).

The Tafel plots were conducted for the cells with the electrodes ( $\text{CoS}_2/\text{C}$  or C) as working electrodes, Na foils as counter electrodes, 25  $\mu\text{L}$   $\text{Na}_2\text{S}_6$  electrolyte, scanning rate of 2  $\text{mV s}^{-1}$ , and the voltage range from 0.8–2.8 V. The exchange current density was obtained by the manually fitted for the linear region of the semi-logarithmic Tafel plot according to the Butler-Volmer equation.

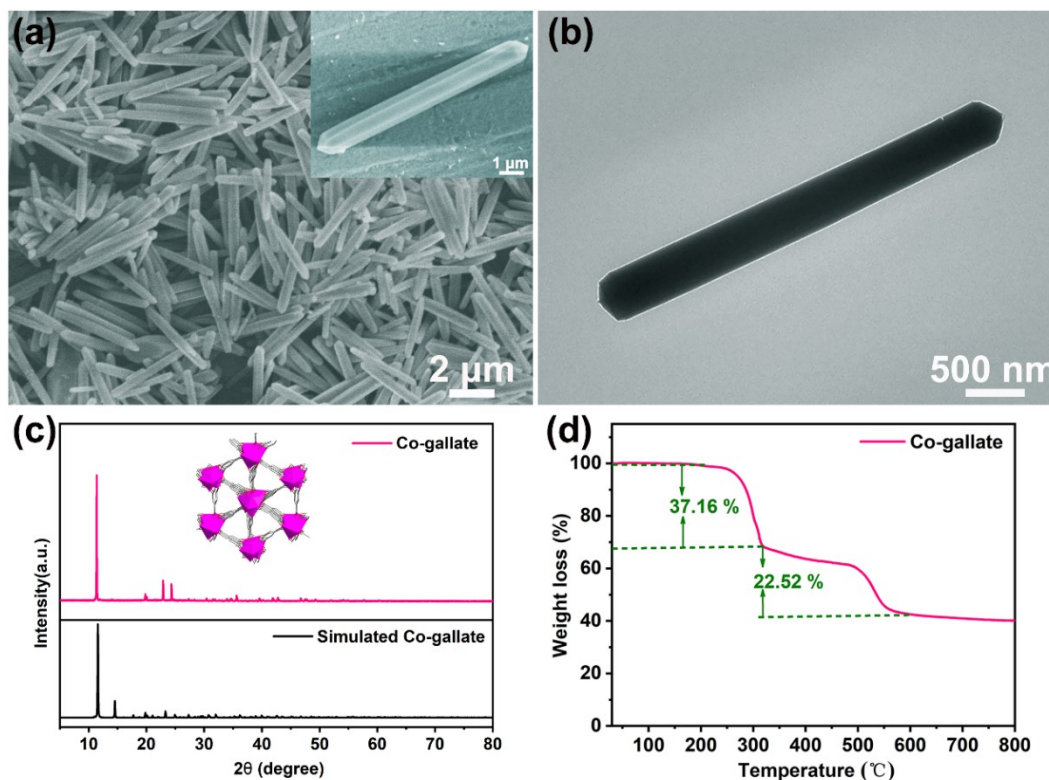


**Fig. S1.** SEM (a) and TEM (b) images of Co-gallate. (c) XRD patterns of Co-gallate.

(d) TGA curve of Co-gallate treated in N<sub>2</sub> with a heating rate of 10 °C min<sup>-1</sup>.

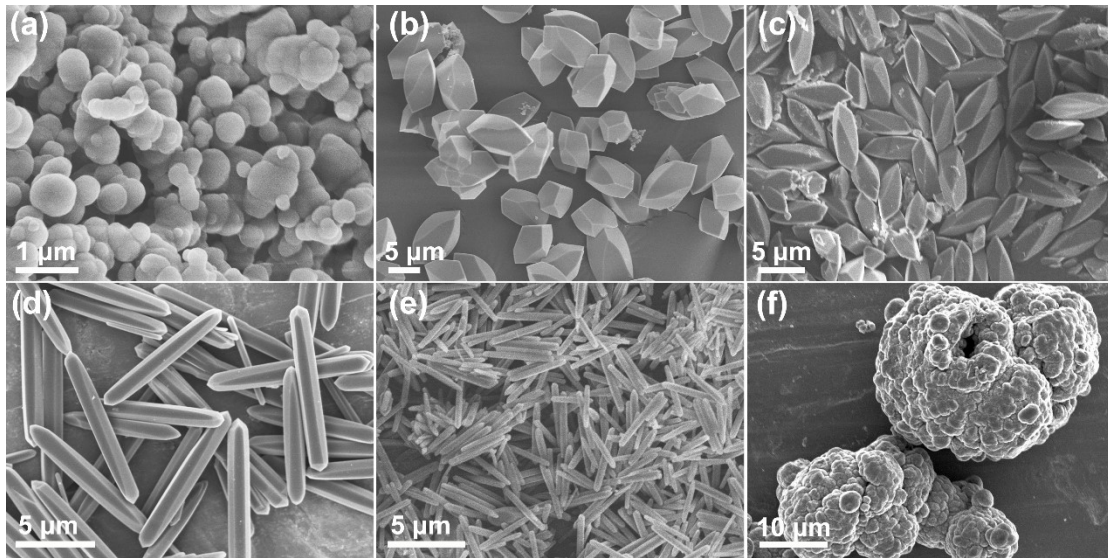


**Fig. S2.** SEM images of Co-gallate after the hydrothermal reaction in different solutions (a) KOH, (b) KOH + anhydrous ethanol and (c) KOH + anhydrous ethanol +ethylene glycol and at different reaction temperatures (d) 120 °C (e) 160 °C and (f) 200 °C for 12 h.

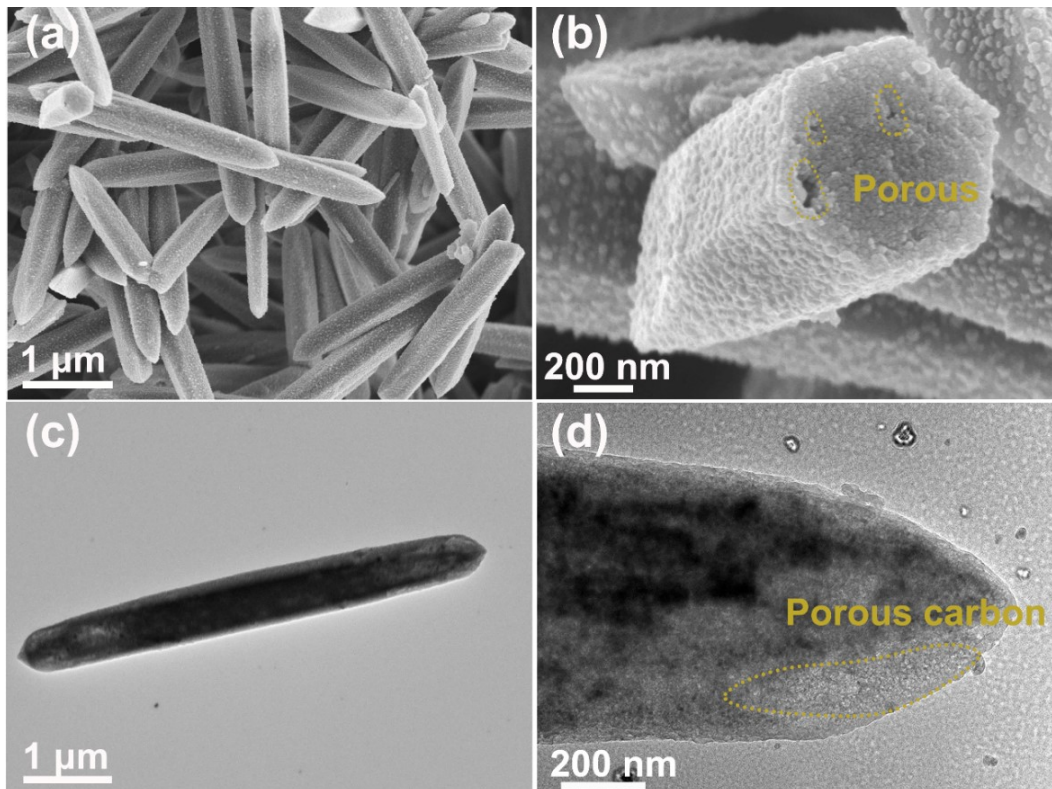


**Fig. S3.** SEM (a, b) and TEM (c, d) images of CoS<sub>2</sub>/C.

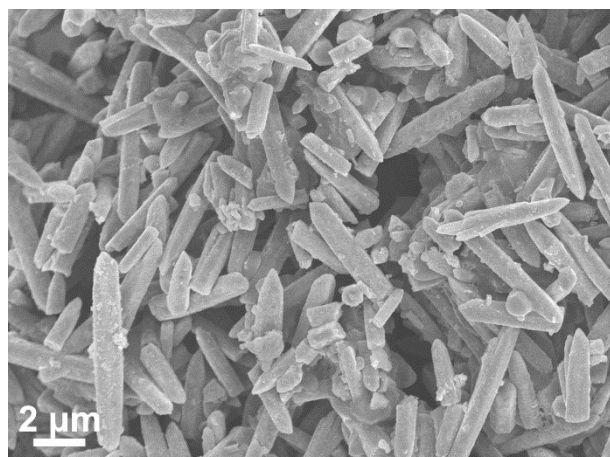


Fig. S4. SEM image of S@CoS<sub>2</sub>/C.

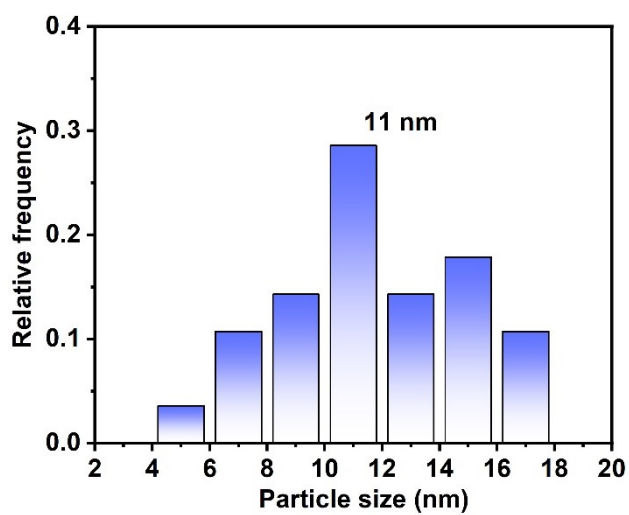


Fig. S5. The normal distribution of particle size of CoS<sub>2</sub> nanoparticles in S@CoS<sub>2</sub>/C.

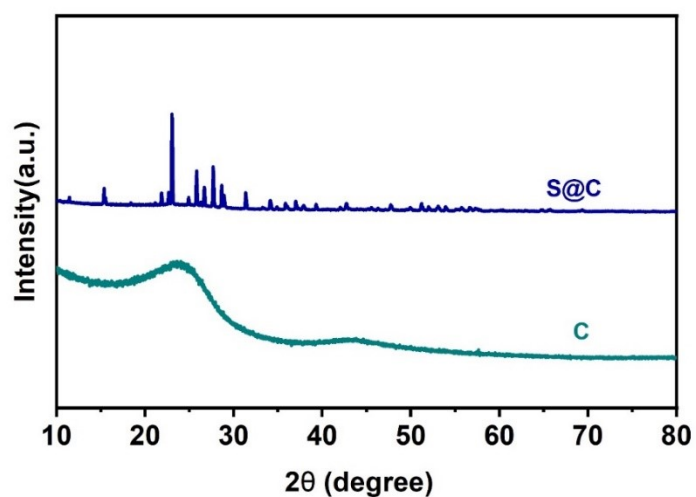


Fig. S6. X-ray diffraction (XRD) patterns of C and S@C.

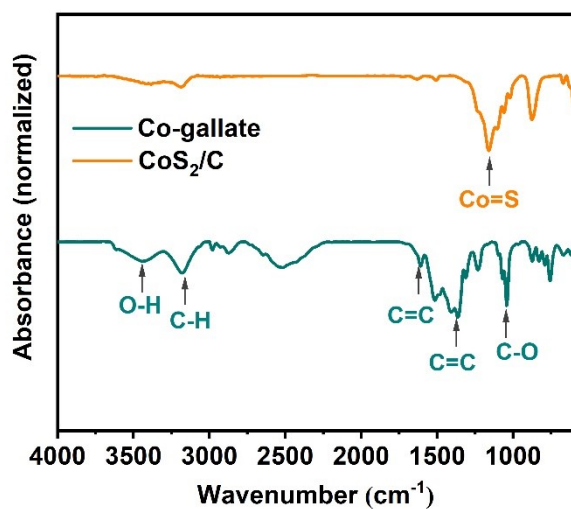


Fig. R7. FTIR spectra of the Co-gallate and CoS<sub>2</sub>/C.

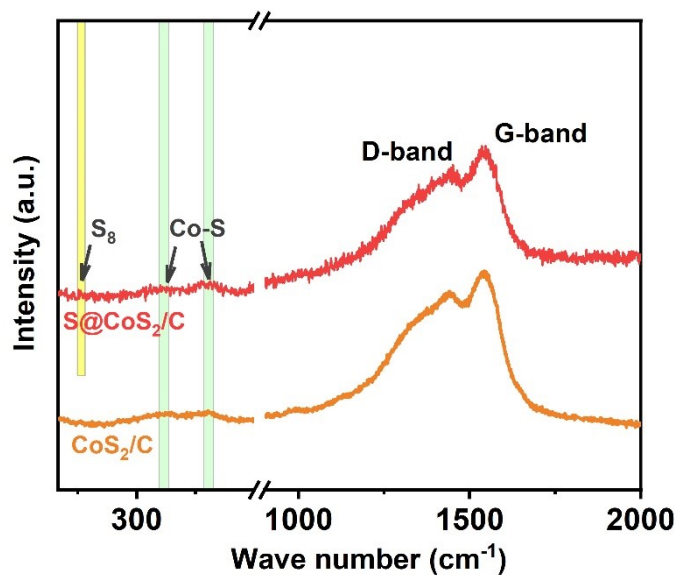
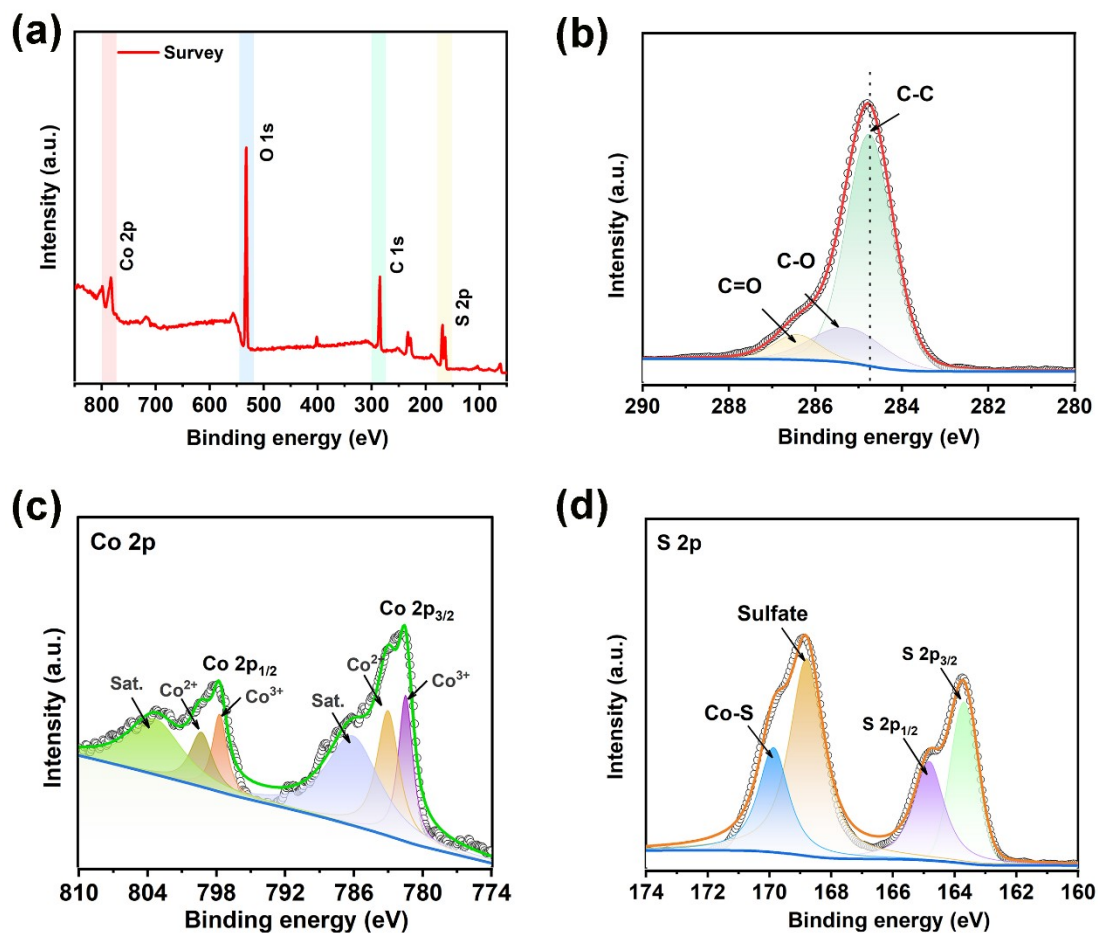
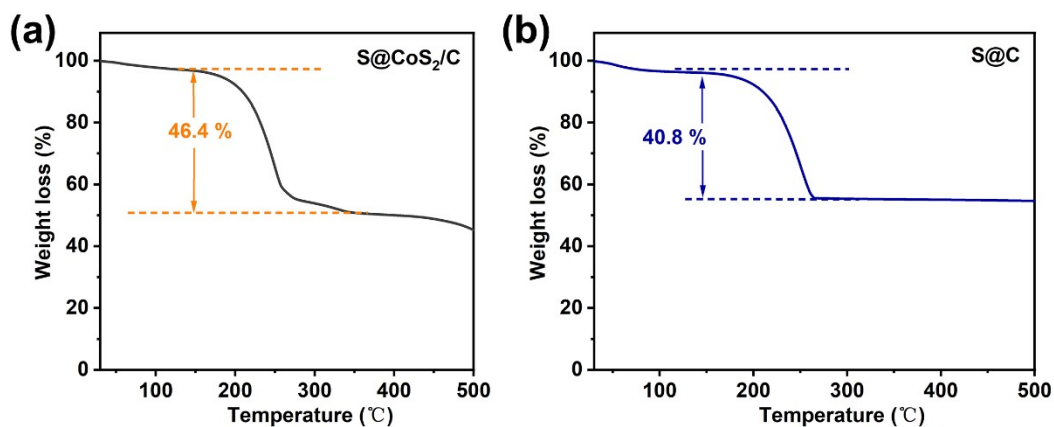


Fig. S8. Raman spectrums of CoS<sub>2</sub>/C and S@CoS<sub>2</sub>/C.



**Fig. S9.** XPS survey spectrum (a) and (b) C of S@CoS<sub>2</sub>/C. High-resolution XPS spectra of (c) Co 2p and (d) S 2p of S@CoS<sub>2</sub>/C.

Note for Fig. S9. The high-resolution C 1s spectrum was fitted with different peaks, with main peaks at binding energy of  $\approx 284.8$  eV related to C-C bonding, which was used as a reference.



**Fig. S10.** TGA curve of the S@CoS<sub>2</sub>/C and S@C composites.



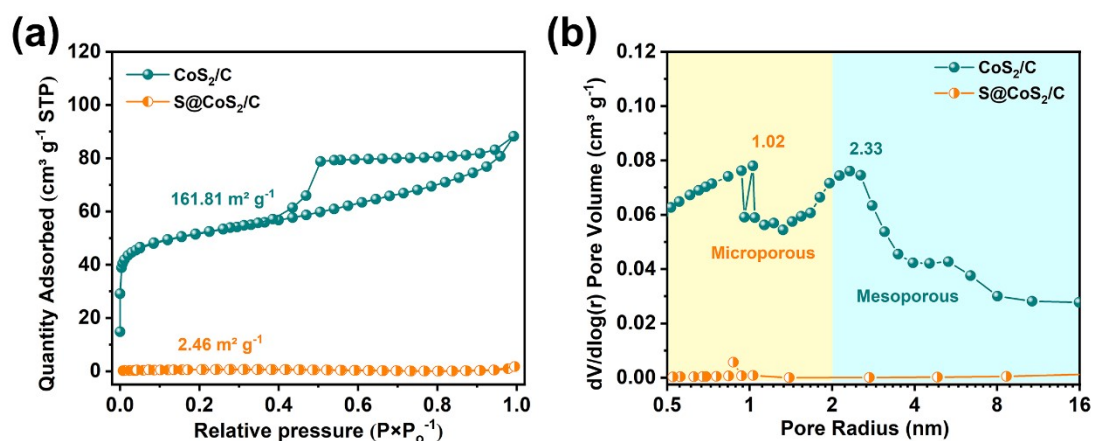


**Fig. S11.** (a) Nitrogen adsorption-desorption isotherms and (b) the corresponding pore size distributions of  $\text{CoS}_2/\text{C}$  and  $\text{S@CoS}_2/\text{C}$ .

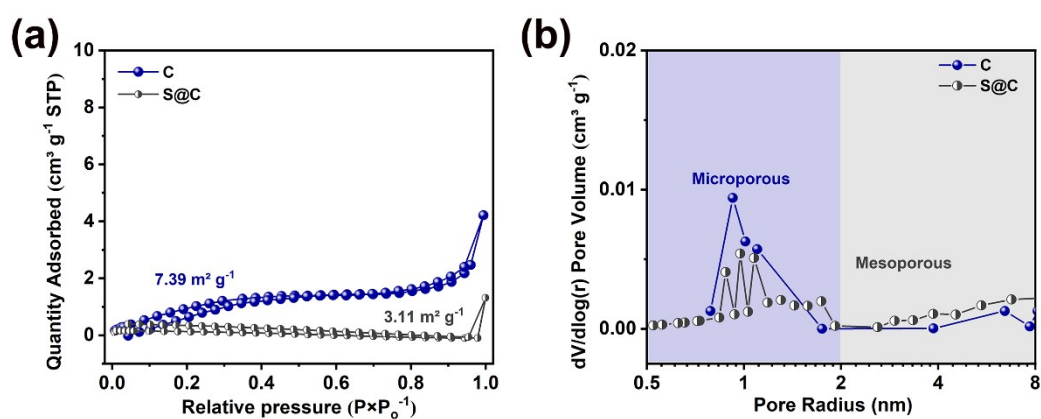


**Fig. S12.** (a) Nitrogen adsorption-desorption isotherms and (b) the corresponding pore size distributions of  $\text{C}$  and  $\text{S@C}$ .

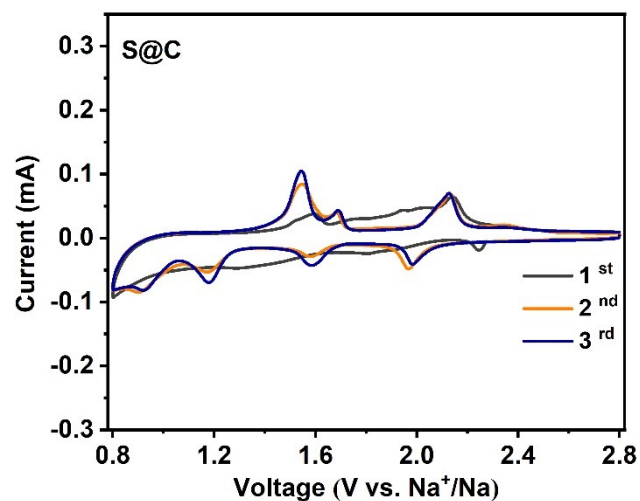


Fig. S13. Cyclic voltammetry curves of the S@C at a scan rate of  $0.1 \text{ mV s}^{-1}$ .

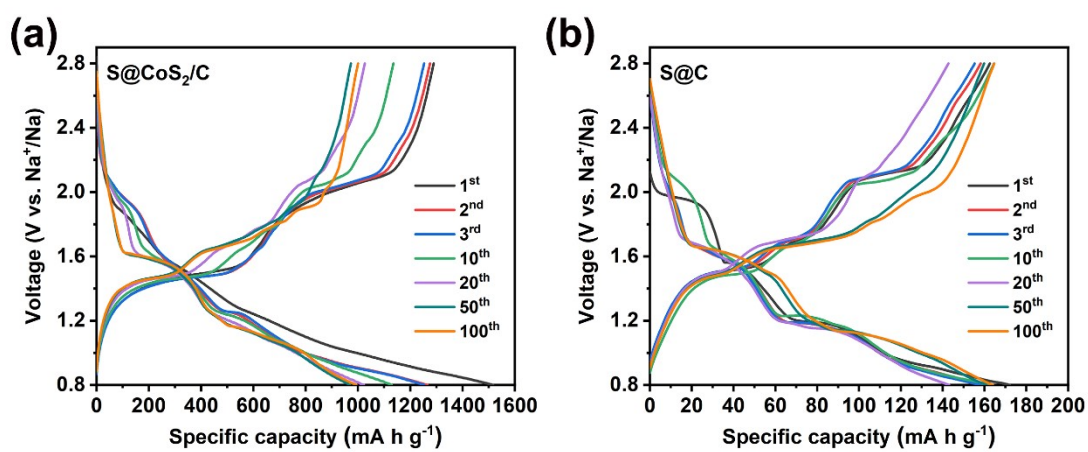
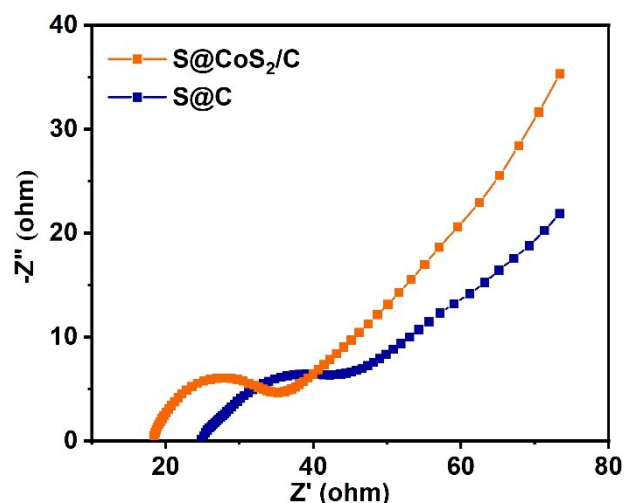
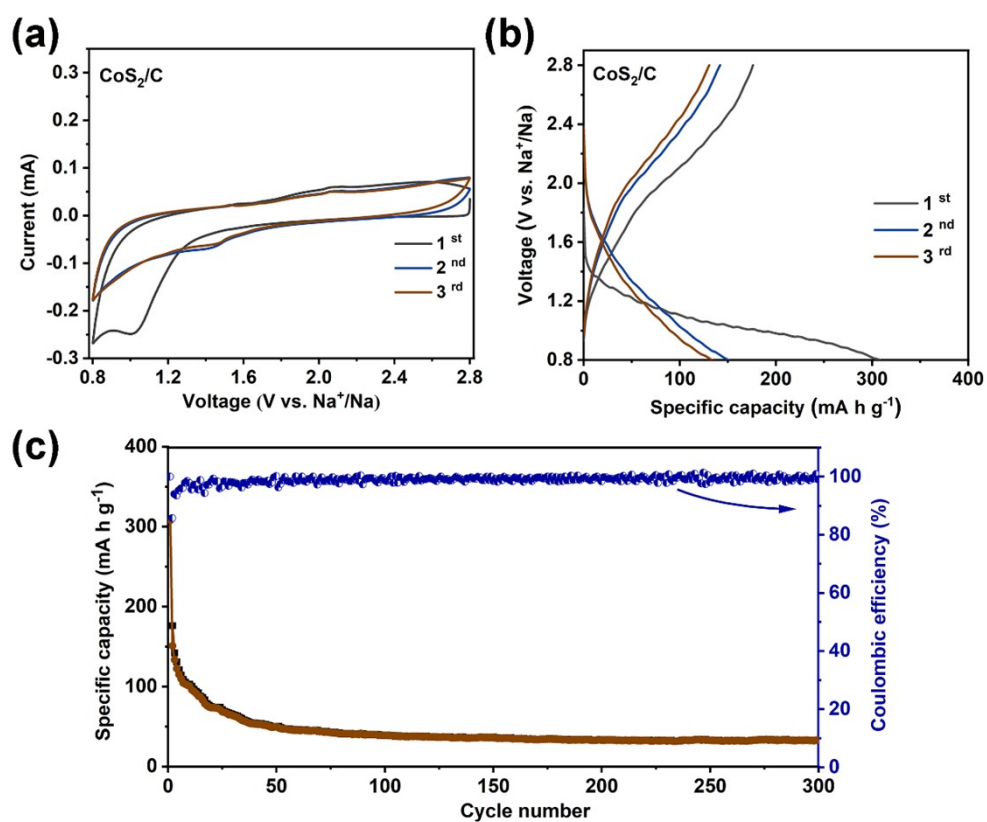


Fig. S14. Galvanostatic charging/discharging curves of different electrodes at  $0.1 \text{ A g}^{-1}$



**Fig. S15.** Nyquist plots of the fresh cells of S@CoS<sub>2</sub>/C and S@C electrodes.

Note to Fig. S15: The semicircle represents the high-frequency region ascribed to the charge-transfer resistance ( $R_{ct}$ ) and the sloping line represents the low-frequency region associated with diffusion of Na<sup>+</sup> in the cathode.<sup>1</sup>



**Fig. S16.** (a) CV curves (b) Charging and discharging curves and (c) cycling performance of pure CoS<sub>2</sub>/C (without sulfur) electrode.

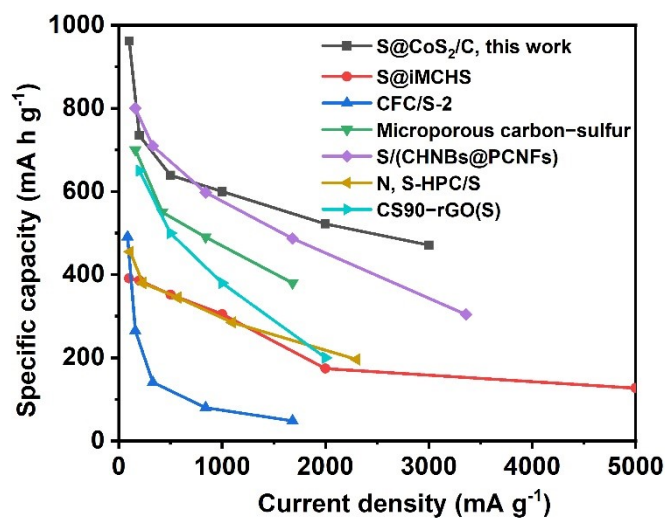


**Fig. S17.** Rate performance of S@CoS<sub>2</sub>/C cell compared to reported counterparts in the literature.

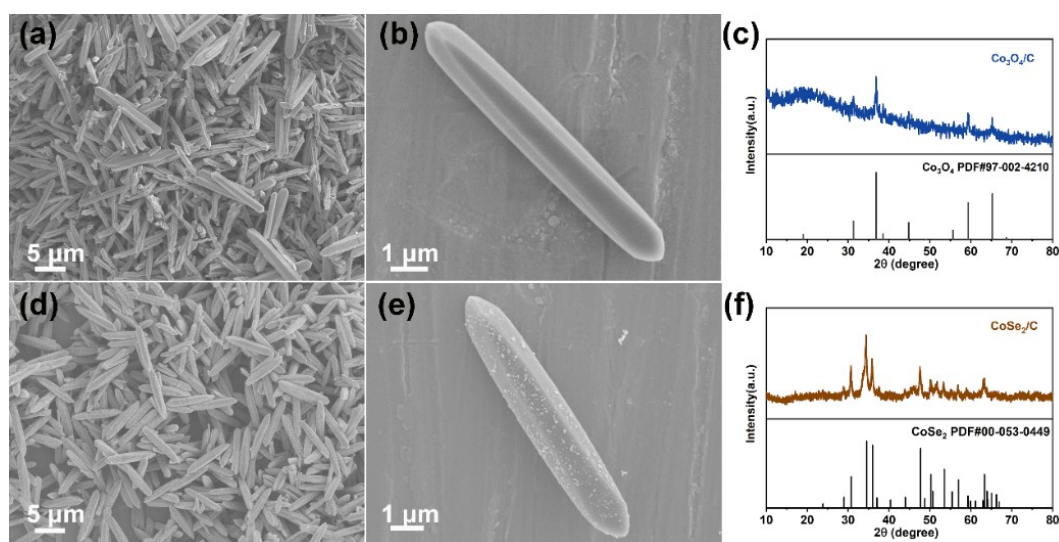


**Fig. S18.** (a, b) SEM images and (c) XRD pattern of Co<sub>3</sub>O<sub>4</sub>/C. (d, e) SEM images and (f) XRD pattern of CoSe<sub>2</sub>/C.

Note for Fig. S18. The SEM of Co<sub>3</sub>O<sub>4</sub>/C and CoSe<sub>2</sub>/C with the same morphology to the Co-gallate precursor were obtained after calcination in the different atmospheres Fig. R2a, b (Co<sub>3</sub>O<sub>4</sub>/C) and Fig. R2d, e (CoSe<sub>2</sub>/C). The XRD pattern shown in Fig. R2c, f additionally confirmed that the phase structure of Co<sub>3</sub>O<sub>4</sub> (PDF # 97-002-4210) and CoSe<sub>2</sub> (PDF # 00-053-0449).

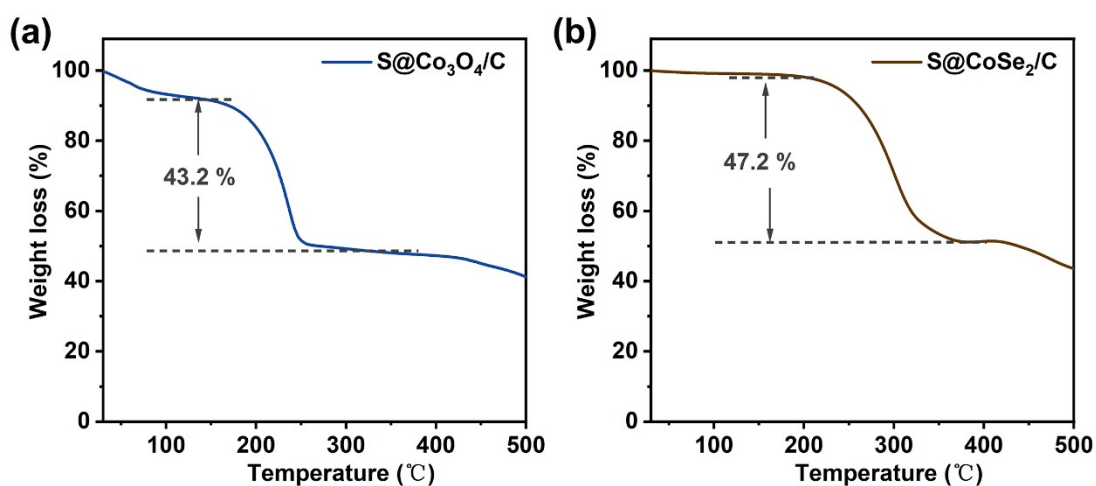


**Fig. S19.** (a, b) Thermogravimetry curves of S@Co<sub>3</sub>O<sub>4</sub>/C and S@CoSe<sub>2</sub>/C, respectively.

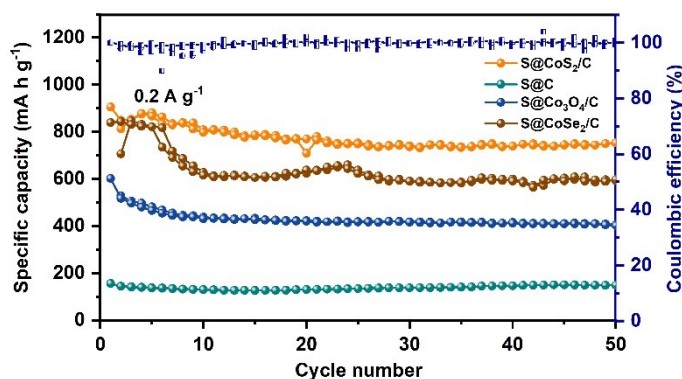


**Fig. S20.** The cycle performance of S@CoS<sub>2</sub>/C, S@C, S@Co<sub>3</sub>O<sub>4</sub>/C and S@CoSe<sub>2</sub>/C cathodes at a current density of 0.2 A g<sup>-1</sup>.

Note for Fig. S20. The S@CoS<sub>2</sub>/C electrode delivers an initial reversible capacity of 905 mA h g<sup>-1</sup>, retaining excellent reversible capacity of 753 mA h g<sup>-1</sup> after 50 cycles. Additionally, the first cycle reversible capacity of S@Co<sub>3</sub>O<sub>4</sub>/C is 602 mA h g<sup>-1</sup>, the capacity is retained 405 mA h g<sup>-1</sup> after 50 cycles. The first cycle reversible capacity of S@CoSe<sub>2</sub>/C is 839 mA h g<sup>-1</sup>, and drops down to 598 mA h g<sup>-1</sup> after 50 cycles. The S@C displays the lowest capacity, which shows the initial reversible capacity of 149 mA h g<sup>-1</sup> after 50 cycles. These results demonstrate that the S@CoS<sub>2</sub>/C electrode demonstrates a greatly improved capacity and long-term cycling performance.

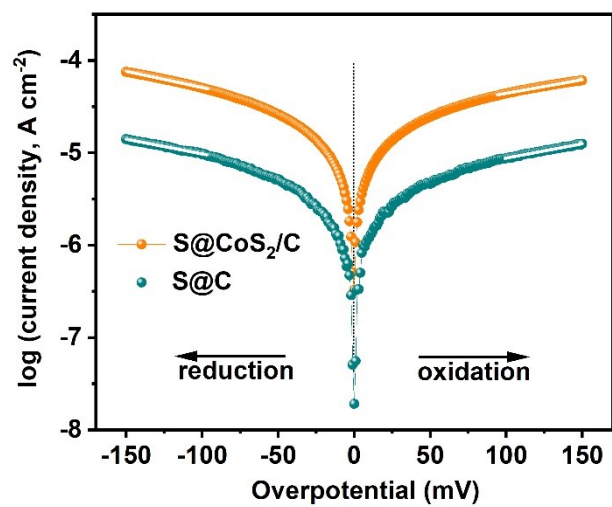


Fig. S21. The Tafel curves for CoS<sub>2</sub>/C and C.

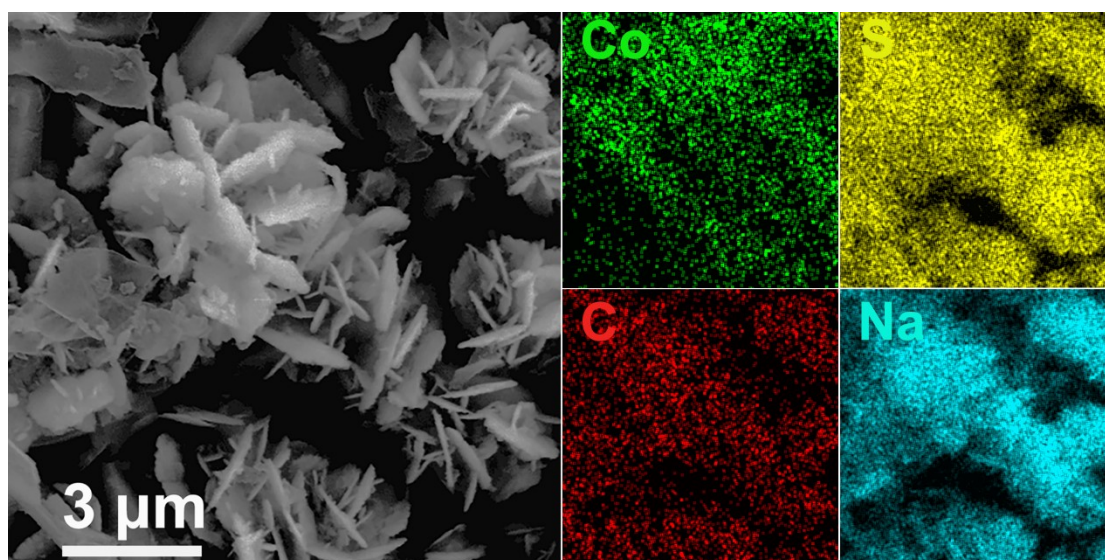
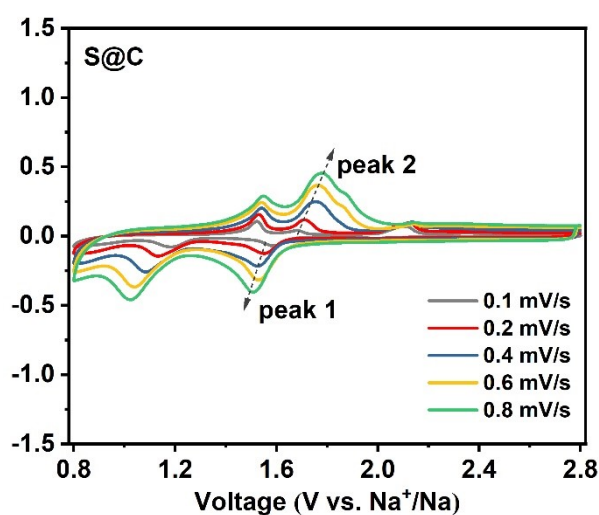


Fig. S22. SEM image and corresponding EDS elemental mappings of electrodeposition test for the CoS<sub>2</sub>/C electrode.



**Fig. S23.** CV curves of S@C at different scan rates from 0.1 to 0.8 mV s<sup>-1</sup>.

**Table S1:** Comparison of this work with previously reported RT Na-S batteries.

Electrode materials	Rate performance	Cycling performance	Ref.
S@CoS <sub>2</sub> /C	471 mA h g <sup>-1</sup> at 3 A g <sup>-1</sup>	623 mA h g <sup>-1</sup> at 1.0 A g <sup>-1</sup> after 870 cycles	This work
S@iMCHS	127 mA h g <sup>-1</sup> at 5 A g <sup>-1</sup>	292 mA h g <sup>-1</sup> at 0.1 A g <sup>-1</sup> after 200 cycles	2
CFC/S-2	48 mA h g <sup>-1</sup> at 1.68 A g <sup>-1</sup>	120 mA h g <sup>-1</sup> at 0.16 A g <sup>-1</sup> after 300 cycles	3
Microporous carbon-sulfur	380 mA h g <sup>-1</sup> at 1.68 A g <sup>-1</sup>	500 mA h g <sup>-1</sup> at 0.16 A g <sup>-1</sup> after 250 cycles	4
S/(CHNBs@P CNFs)	304 mA h g <sup>-1</sup> at 3.36 A g <sup>-1</sup>	786 mA h g <sup>-1</sup> at 0.16 A g <sup>-1</sup> after 50 cycles	5
N, S-HPC/S	196 mA h g <sup>-1</sup> at 2.3 A g <sup>-1</sup>	378 mA h g <sup>-1</sup> at 0.23 A g <sup>-1</sup> after 250 cycles	6
CS90-rGO(S)	200 mA h g <sup>-1</sup> at 2 A g <sup>-1</sup>	285 mA h g <sup>-1</sup> at 1.0 A g <sup>-1</sup> after 100 cycles	7

## References

1. J. Zhang, C.-P. Yang, Y.-X. Yin, L.-J. Wan and Y.-G. Guo, *Adv. Mater.*, 2016, **28**, 9539–9544.
2. Y. X. Wang, J. Yang, W. Lai, S. L. Chou, Q. F. Gu, H. K. Liu, D. Zhao and S. X. Dou, *J. Am. Chem. Soc.*, 2016, **138**, 16576-16579.
3. X. W. Qionqiong Lu, Jun Cao, Chen Chen, Kena Chen, Zifang Zhao, Zhiqiang Niu, Jun Chen, *Energy Storage Materials*, 2017, **8**, 77–84.
4. R. Carter, L. Oakes, A. Douglas, N. Muralidharan, A. P. Cohn and C. L. Pint, *Nano Lett.*, 2017, **17**, 1863-1869.
5. G. Xia, L. Zhang, X. Chen, Y. Huang, D. Sun, F. Fang, Z. Guo and X. Yu, *Energy Storage Materials*, 2018, **14**, 314-323.
6. Z. Qiang, Y.-M. Chen, Y. Xia, W. Liang, Y. Zhu and B. D. Vogt, *Nano Energy*, 2017, **32**, 59-66.
7. A. Ghosh, S. Shukla, M. Monisha, A. Kumar, B. Lochab and S. Mitra, *ACS Energy Letters*, 2017, **2**, 2478-2485.